Pentadienyl–Metal–Phosphine Chemistry. 15.[1] Synthesis, Structure, and Reactivity of (η^5-Pentadienyl)(η^3-pentadienyl)Fe(PR_3) Complexes

John R. Bleeke,* Mary K. Hays, and Robert J. Wittenbrink

Department of Chemistry, Washington University, St. Louis, Missouri 63130

Received December 9, 1987

Reaction of $FeCl_2(PMe_3)_2$ with 2 equiv of potassium pentadienide (K^+pd^-) produces (η^3-pd)$_2$Fe(PMe_3)$_2$ (**1**). Upon refluxing in diethyl ether, **1** slowly loses PMe_3 and is converted to (η^5-pd)(η^3-pd)Fe(PMe_3) (**2**). The PEt_3 and P-*n*-Pr_3 analogues of **2**, (η^5-pd)(η^3-pd)Fe(PEt_3) (**3**) and (η^5-pd)(η^3-pd)Fe(P-*n*-Pr_3) (**4**), are obtained directly upon reaction of the appropriate $FeCl_2(PR_3)_2$ reagent with 2 equiv of K^+pd^-. **3** crystallizes in the triclinic space group $P\bar{1}$ with a = 9.762 (6) Å, b = 10.136 (5) Å, c = 9.271 (5) Å, α = 97.95 (2)°, β = 111.56 (4)°, γ = 92.26 (4)°, V = 840.8 (7) Å^3, and Z = 2. The η^5-pentadienyl ligand in **2** is U-shaped, while the η^3-pd ligand is bonded in a W-shaped syn geometry. The η^3-pentadienyl ligand assumes an exo rotational orientation with respect to the η^5-pd ligand. Compounds **3** and **4** react with excess PMe_3 in refluxing diethyl ether to produce **1**. When **3** and **4** are refluxed in diethyl ether in the *absence* of PMe_3, the pentadienyl ligands couple stereoselectively to produce (η^8-*trans,trans*-1,3,7,9-decatetraene)Fe(PEt_3) (**5**) and (η^8-*trans,trans*-1,3,7,9-decatetraene)Fe(P-*n*-Pr_3) (**6**), respectively. **5** crystallizes in the monoclinic space group $P2_1/n$ with a = 7.434 (4) Å, b = 27.536 (3) Å, c = 7.662 (1) Å, β = 93.112 (3)°, V = 1566 (1) Å^3, and Z = 4. The two butadiene moieties of the decatetraene ligand are bonded to the Fe center in a cisoid fashion and are eclipsed. Compound **3** is converted to (η^5-pd)Fe(PMe_3)$_3^+X^-$ (**7a**, X^- = BF_4^-; **7b**, X^- = PF_6^-) and (η^5-pd)Fe[(Me_2PCH_2)$_3$CMe]$^+X^-$ (**8a**, X = BF_4^-; **8b**, X^- = PF_6^-) upon treatment with $HX{\cdot}OEt_2$ or Ag^+X^-, followed by addition of the appropriate phosphine reagent. **7a** crystallizes in the monoclinic space group $P2_1/c$ with a = 9.697 (2) Å, b = 12.923 (4) Å, c = 16.834 (4) Å, β = 90.48 (2)°, V = 2109.6 (9) Å^3, and Z = 4. The coordination geometry of **7a** is pseudooctahedral; one phosphorus atom resides under the open "mouth" and the other two reside in sites under the "edges" of the pd ligand. **7** and **8** undergo dynamic processes in solution, involving rotation of the pd ligand with respect to the FeP_3 framework. Treatment of **3** with $HX{\cdot}OEt_2$ or Ag^+X^-, followed by addition of P(OMe)$_3$, produces (η^5-pd)Fe[P(OMe)$_3$]$_2$(PEt_3)$^+X^-$ (**9a**, X^- = BF_4^-; **9b**, X^- = PF_6^-). In solution, **9** exists as an equilibrium mixture of two isomers—a symmetrical isomer in which the PEt_3 ligand resides under the "mouth" of the pd ligand and an unsymmetrical isomer in which PEt_3 resides under a pd "edge". These isomers interconvert via pentadienyl ligand rotation.

Introduction

Electron-rich organometallic complexes containing polyene or polyenyl ligands have recently attracted considerable attention because of their ability to (a) react with small organic molecules such as CH_4 and CO_2,[2] (b) stabilize unusual bonding interactions such as three-center C–H–M interactions,[3] and (c) undergo oxidation to yield novel radical species.[4] Furthermore, these compounds have potential utility in organic synthesis because their electron-richness influences the regiochemistry of nucleophilic addition to the polyene or polyenyl ligand.[5]

Our efforts in this area have been focussed on transition metal–phosphine complexes containing the acyclic pentadienyl (pd) ligand, a class of compounds whose reactivity is further enhanced by the accessibility of a variety of pd bonding modes (η^5, η^3, and η^1).[6] In an earlier communi-

Scheme I[a]

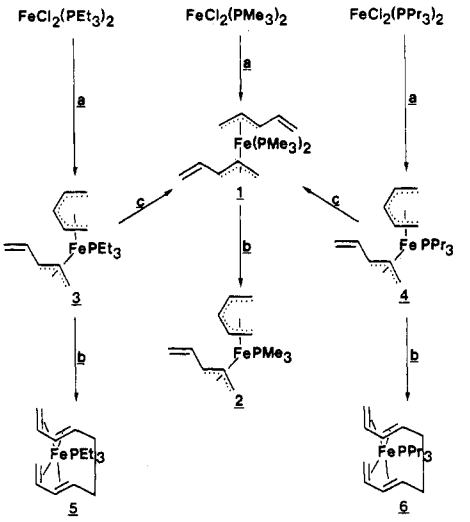

[a] (a) 2 equiv of potassium pentadienide; (b) refluxing OEt_2; (c) 5 equiv of PMe_3 in refluxing OEt_2.

(1) The previous papers in this series are as follows: (a) Bleeke, J. R.; Kotyk, J. J. *Organometallics* **1983**, *2*, 1263. (b) Bleeke, J. R.; Hays, M. K. *Ibid.* **1984**, *3*, 506. (c) Bleeke, J. R.; Peng, W.-J. *Ibid.* **1984**, *3*, 1422. (d) Bleeke, J. R.; Kotyk, J. J. *Ibid.* **1985**, *4*, 194. (e) Bleeke, J. R.; Peng, W.-J. *Ibid.* **1986**, *5*, 635. (f) Bleeke, J. R.; Stanley, G. G.; Kotyk, J. J. *Ibid.* **1986**, *5*, 1642. (g) Bleeke, J. R.; Moore, D. A. *Inorg. Chem.* **1986**, *25*, 3522. (h) Bleeke, J. R.; Donaldson, A. J. *Organometallics* **1986**, *5*, 2401. (i) Bleeke, J. R.; Hays, M. K. *Ibid.* **1987**, *6*, 486. (j) Bleeke, J. R.; Kotyk, J. J.; Moore, D. A.; Rauscher, D. J. *J. Am. Chem. Soc.* **1987**, *109*, 417. (k) Bleeke, J. R.; Hays, M. K. *Organometallics* **1987**, *6*, 1367. (l) Bleeke, J. R.; Peng, W.-J. *Ibid.* **1987**, *6*, 1576. (m) Bleeke, J. R.; Donaldson, A. J.; Peng, W.-J. *Ibid.* **1988**, *7*, 33. (n) Bleeke, J. R.; Rauscher, D. J.; Moore, D. A. *Ibid.* **1987**, *6*, 2614.

(2) See, for example: (a) Janowicz, A. H.; Bergman, R. G. *J. Am. Chem. Soc.* **1983**, *105*, 3929. (b) Jones, W. D.; Feher, F. *Ibid.* **1984**, *106*, 1650. (c) Bergman, R. G.; Seidler, P. F.; Wenzel, T. T. *Ibid.* **1985**, *107*, 4358. (d) Green, M. L. H.; Joyner, D. S.; Wallis, J.; Bell, J. P. 190th National Meeting, American Chemical Society, Chicago, IL (Sept. 1985). (e) Hoberg, H.; Jenni, K.; Krüger, C.; Raabe, E. *Angew. Chem., Int. Ed. Engl.* **1986**, *25*, 810.

(3) See, for example: (a) Ittel, S. D.; Van-Catledge, F. A.; Jesson, J. P. *J. Am. Chem. Soc.* **1979**, *101*, 6905. (b) Schultz, A. J.; Brown, R. K.; Williams, J. M.; Schrock, R. *Ibid.* **1981**, *103*, 169. (c) Dawoodi, Z.; Green, M. L. H.; Mtetwa, V. S. B.; Prout, K. *J. Chem. Soc., Chem. Commun.* **1982**, 1410. (d) Cracknell, R. B.; Orpen, A. G.; Spencer, J. L. *Ibid.* **1984**, 326. (e) Brookhart, M.; Green, M. L. H. *J. Organomet. Chem.* **1983**, *250*, 395 and references cited therein.

(4) See, for example: (a) Hayes, J. C.; Cooper, N. J. *J. Am. Chem. Soc.* **1982**, *104*, 5570. (b) Harlow, R. L.; McKinney, R. J.; Witney, J. F. *Organometallics* **1983**, *2*, 1839. (c) Reference 1e.

(5) (a) Davies, S. G.; Green, M. L. H.; Mingos, D. M. P. *Tetrahedron* **1978**, *34*, 3047. (b) Reference 1l.

0276-7333/88/2307-1417$01.50/0

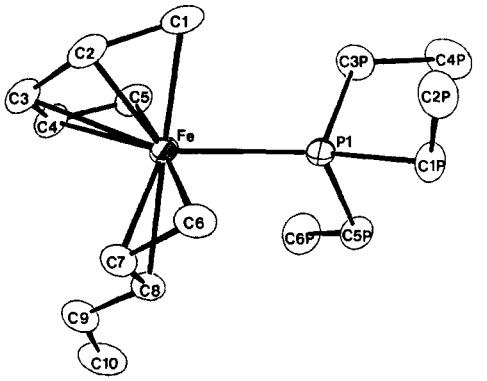

Figure 1. ORTEP drawing of (η^5-pentadienyl)(η^3-pentadienyl)-Fe(PEt_3) (**3**). Hydrogen atoms are omitted for clarity.

cation, we described the synthesis of (η^3-pd)$_2$Fe(PMe_3)$_2$ (**1**) from the reaction of $FeCl_2(PMe_3)_2$ with 2 equiv of potassium pentadienide.[1b] We now report that upon prolonged heating in diethyl ether, **1** loses PMe_3 and is converted to (η^5-pd)(η^3-pd)Fe(PMe_3) (**2**). In addition, the PEt_3 and P-*n*-Pr_3 analogues of **2**, (η^5-pd)(η^3-pd)Fe(PEt_3) (**3**) and (η^5-pd)(η^3-pd)Fe(P-*n*-Pr_3) (**4**), can be obtained directly upon reaction of the appropriate $FeCl_2(PR_3)_2$ reagent with 2 equiv of K^+pd^-. Complexes **3** and **4** undergo several important reactions, including stereoselective pentadienyl coupling to generate (η^8-*trans,trans*-1,3,7,9-decatetraene)Fe(PR_3) products and clean conversion to a variety of (η^5-pd)$FeL_3^+X^-$ complexes.

Results and Discussion

A. Synthesis of (η^5-Pentadienyl)(η^3-pentadienyl)-Fe(PR_3) Complexes. Earlier, we reported the synthesis of (η^3-pentadienyl)$_2$Fe(PMe_3)$_2$ (**1**) from the reaction of $FeCl_2(PMe_3)_2$ with 2 equiv of potassium pentadienide.[1b] We now find that **1** is converted to (η^5-pentadienyl)(η^3-pentadienyl)Fe(PMe_3) (**2**) upon refluxing in diethyl ether for several days (see Scheme I). Furthermore, **2** is not reconverted to **1** upon treatment with excess PMe_3. These observations clearly indicate that **1** is the kinetic product and **2** is the thermodynamic product in this system.

Treatment of $FeCl_2(PEt_3)_2$ and $FeCl_2$(P-*n*-$Pr_3)_2$ with 2 equiv of potassium pentadienide (K^+pd^-) produces (η^5-pd)(η^3-pd)Fe(PEt_3) (**3**) and (η^5-pd)(η^3-pd)Fe(P-*n*-Pr_3) (**4**) directly. In these reactions involving relatively bulky phosphines,[7] the kinetic products [(η^3-pd)$_2$Fe(PR_3)$_2$] are probably too sterically congested to be isolable.

B. Structure and Spectroscopy of (η^5-Pentadienyl)(η^3-pentadienyl)Fe(PR_3) Complexes. The molecular structure of **3** (Figure 1) has been obtained from a single-crystal X-ray diffraction study. Positional parameters of non-hydrogen atoms are listed in Table I, while selected bond distances and angles are given in Table II. The complex adopts an approximately octahedral coordination geometry with C1, C3, C5, C6, C8, and P1 occupying the six coordination sites. The η^5-pentadienyl ligand is planar and U-shaped, while the η^3-pd ligand is bonded in a W-shaped (syn) geometry. Furthermore, the η^3-pentadienyl ligand assumes an exo rotational orientation; i.e., its "mouth" points down (away from) the η^5-pd ligand. This preference for the exo orientation probably results from the very small dihedral angle (14°) that the η^3-pentadienyl plane makes with the η^5-pentadienyl plane in this geometry. A substantially larger dihedral angle (58°), together with greater steric interactions, is anticipated for the endo rotamer.[8]

Table I. Positional Parameters and Their Estimated Standard Deviations for Non-Hydrogen Atoms in (η^5-Pentadienyl)(η^3-pentadienyl)Fe(PEt_3) (3)

atom	*x*	*y*	*z*
Fe	0.31648 (7)	0.25342 (6)	0.18016 (6)
P1	0.1915 (1)	0.2664 (1)	0.3410 (1)
C1	0.2705 (7)	0.0431 (5)	0.1395 (6)
C2	0.3733 (6)	0.0829 (5)	0.0781 (6)
C3	0.3499 (6)	0.1794 (6)	−0.0247 (6)
C4	0.2335 (7)	0.2597 (6)	−0.0581 (5)
C5	0.1137 (6)	0.2460 (6)	−0.0118 (6)
C6	0.5220 (6)	0.2806 (5)	0.3688 (6)
C7	0.5070 (5)	0.3727 (5)	0.2660 (6)
C8	0.4001 (5)	0.4645 (5)	0.2497 (5)
C9	0.3735 (6)	0.5572 (5)	0.1364 (6)
C10	0.3101 (8)	0.6700 (6)	0.1429 (8)
C1P	0.2796 (6)	0.2275 (5)	0.5406 (5)
C2P	0.3437 (7)	0.0940 (6)	0.5515 (6)
C3P	0.0162 (6)	0.1557 (6)	0.2660 (7)
C4P	−0.0809 (7)	0.1634 (9)	0.3616 (9)
C5P	0.1307 (5)	0.4299 (5)	0.3968 (5)
C6P	0.0334 (7)	0.4924 (6)	0.2626 (8)

Table II. Bond Distances (Å) and Bond Angles (deg) with Estimated Standard Deviations for (η^5-Pentadienyl)(η^3-pentadienyl)Fe(PEt_3) (3)

Bond Distances

Fe–P1	2.242 (1)	Fe–C8	2.180 (3)	C9–C10	1.326 (7)
Fe–C1	2.113 (4)	C1–C2	1.395 (7)	P1–C1P	1.838 (4)
Fe–C2	2.049 (4)	C2–C3	1.426 (6)	P1–C3P	1.852 (4)
Fe–C3	2.088 (4)	C3–C4	1.391 (7)	P1–C5P	1.853 (4)
Fe–C4	2.066 (4)	C4–C5	1.395 (7)	C1P–C2P	1.514 (6)
Fe–C5	2.110 (4)	C6–C7	1.399 (6)	C3P–C4P	1.515 (8)
Fe–C6	2.098 (4)	C7–C8	1.406 (6)	C5P–C6P	1.500 (7)
Fe–C7	2.066 (4)	C8–C9	1.464 (6)		

Bond Angles

P1–Fe–C1	88.4 (1)	C3–Fe–C6	108.3 (2)	C8–C9–C10	125.6 (6)
P1–Fe–C3	154.1 (1)	C3–Fe–C8	108.5 (2)	Fe–P1–C1P	119.7 (1)
P1–Fe–C5	88.9 (1)	C5–Fe–C6	174.3 (2)	Fe–P1–C3P	114.6 (2)
P1–Fe–C6	92.5 (1)	C5–Fe–C8	105.3 (2)	Fe–P1–C5P	118.8 (1)
P1–Fe–C8	93.1 (2)	C6–Fe–C8	69.1 (2)	C1P–P1–C3P	101.4 (2)
C1–Fe–C3	72.7 (2)	C1–C2–C3	123.9 (5)	C1P–P1–C5P	97.2 (2)
C1–Fe–C5	84.1 (2)	C2–C3–C4	124.6 (4)	C3P–P1–C5P	101.9 (2)
C1–Fe–C6	101.5 (2)	C3–C4–C5	124.8 (4)	P1–C1P–C2P	115.7 (4)
C1–Fe–C8	170.5 (2)	C6–C7–C8	119.9 (4)	P1–C3P–C4P	118.6 (4)
C3–Fe–C5	72.0 (2)	C7–C8–C9	121.9 (4)	P1–C5P–C6P	115.5 (3)

The syn-exo orientation of the η^3-pd ligand in **3** appears to be retained in solution. Particularly diagnostic is the substantial shielding exhibited by anti protons $H6_{anti}$ (δ −0.45) and H8 (δ 0.76) in the ^1H NMR spectrum[8,9] (see drawing for numbering scheme).

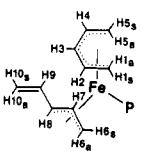

The striking similarity of the NMR specta of **2** and **4** to those of **3** strongly suggests that the η^3-pd ligands in these complexes also adopt the syn-exo orientation.

C. Reactions of 3 and 4 with PMe_3. As indicated in Scheme I, both **3** and **4** react irreversibly with excess PMe_3 in refluxing diethyl ether to produce (η^3-pd)$_2$Fe(PMe_3)$_2$ (**1**). (Recall that **2** does not undergo this reaction.) We propose (Scheme II) that this reaction proceeds by initial slippage of the η^5-pd ligand to an η^3-bonding mode, generating a

(6) See also: (a) Ernst, R. D. *Acc. Chem. Res.* **1985**, *18*, 56. (b) Powell, P. *Adv. Organomet. Chem.* **1986**, *26*, 125. (c) Lush, S.-F.; Liu, R.-S. *Organometallics* **1986**, *5*, 1908.

(7) PEt_3 and P-*n*-Pr_3 have cone angles of 132° compared to a cone angle of 118° for PMe_3: Tolman, C. A. *Chem. Rev.* **1977**, *77*, 313.

(8) Fish, R. W.; Giering, W. P.; Marten, D.; Rosenblum, M. *J. Organomet. Chem.* **1976**, *105*, 101.

(9) Gibson, D. H.; Hsu, W.-L.; Steinmetz, A. L.; Johnson, B. V. *J. Organomet. Chem.* **1981**, *208*, 89.

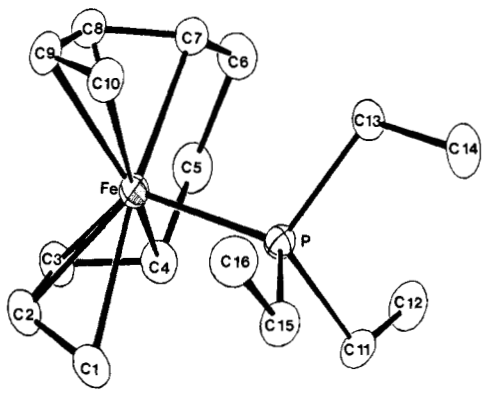

Figure 2. ORTEP drawing of (η^8-1,3,7,9-decatetraene)Fe(PEt_3) (**5**). Hydrogen atoms are omitted for clarity.

Scheme II[a]

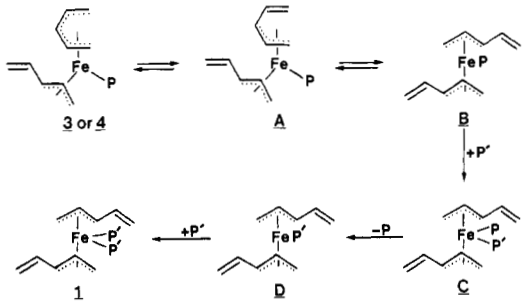

[a] P = PEt_3 or P-*n*-Pr_3; P′ = PMe_3.

16e intermediate (A, B), which coordinates PMe_3. The resulting sterically crowded intermediate (C) relieves strain by losing the larger phosphine (PEt_3 or P-*n*-Pr_3) and then rapidly coordinates a second PMe_3 ligand, producing **1**. The initial pentadienyl slippage is apparently promoted by the presence of the bulky phosphines, PEt_3 and P-*n*-Pr_3.

D. Coupling of the Pentadienyl Ligands in 3 and 4. Synthesis, Structure, and Spectroscopy of (η^8-1,3,7,9-Decatetraene)Fe(PEt_3) (5) and (η^8-1,3,7,9-Decatetraene)Fe(P-*n*-Pr_3)$_3$ (6). When **3** and **4** are refluxed in diethyl ether in the absence of added PMe_3, the pentadienyl ligands couple[10] to produce (η^8-1,3,7,9-decatetraene)Fe(PEt_3) (**5**) and (η^8-1,3,5,7-decatetraene)Fe(P-*n*-Pr_3) (**6**), respectively.[11] The molecular structure of **5** (Figure 2) has been determined by single-crystal X-ray diffraction. Positional parameters of non-hydrogen atoms are listed in Table III, while selected bond distances and angles are given in Table IV. The structure of **5** closely resembles that of (η^8-2,4,7,9-tetramethyl-1,3,7,9-decatetraene)Mn(PMe_3), which we reported earlier.[1a] Its geometry is square-pyramidal with the four C–C bonds of the decatetraene ligand occupying the basal sites and the phosphorus atom of the PEt_3 ligand occupying the axial site. The two butadiene moieties of the decatetraene ligand are bonded to the metal in a cisoid fashion[12] and are fully eclipsed. The butadiene planes intersect with a dihedral angle of 14.2°. Significantly, the two internal double bonds of the decatetraene ligand have trans configurations. This trans,trans stereochemistry demands that the coupling occur from a bis(*syn*-η^3-pd) intermediate, as shown in Scheme III, because coupling of an anti (U-shaped) pentadienyl ligand (η^3 or η^5) would result in cis double-bond stereochemistry in the decatetraene product.

In solution, **5** and **6** exhibit mirror-plane symmetry. Hence, the decatetraene ligand gives rise to only five signals in the $^{13}C\{^1H\}$ NMR spectrum and seven signals ($H1_{anti}$, $H1_{syn}$, H2, H3, H4, $H5_{anti}$, $H5_{syn}$) in the ^1H NMR spectrum. As expected for the trans,trans geometry, the

Table III. Positional Parameters and Their Estimated Standard Deviations for Non-Hydrogen Atoms in (η^8-1,3,7,9-Decatetraene)Fe(PEt_3) (5)

atom	*x*	*y*	*z*
Fe	0.09153 (5)	0.15955 (1)	0.13614 (5)
P	0.25975 (9)	0.09396 (2)	0.20099 (9)
C1	0.2939 (4)	0.1752 (1)	−0.0384 (4)
C2	0.1818 (4)	0.2151 (1)	−0.0132 (5)
C3	0.1559 (4)	0.2312 (1)	0.1597 (5)
C4	0.2315 (4)	0.2059 (1)	0.3074 (4)
C5	0.1380 (5)	0.2117 (1)	0.4790 (5)
C6	0.0106 (5)	0.1688 (1)	0.5127 (4)
C7	−0.0660 (4)	0.1473 (1)	0.3428 (4)
C8	−0.1555 (4)	0.1771 (1)	0.2153 (4)
C9	−0.1685 (4)	0.1612 (1)	0.0387 (5)
C10	−0.1014 (4)	0.1154 (1)	−0.0057 (4)
C11	0.4761 (4)	0.1016 (1)	0.3285 (4)
C12	0.4699 (5)	0.1138 (1)	0.5212 (5)
C13	0.1530 (4)	0.0450 (1)	0.3224 (4)
C14	0.2545 (5)	−0.0029 (1)	0.3485 (6)
C15	0.3529 (4)	0.0606 (1)	0.0167 (4)
C16	0.2185 (6)	0.0391 (1)	−0.1180 (5)

Table IV. Bond Distances (Å) and Bond Angles (deg) with Estimated Standard Deviations for (η^8-1,3,7,9-Decatetraene)Fe(PEt_3) (5)

Bond Distances					
Fe–P	2.2372 (6)	Fe–C10	2.132 (3)	C8–C9	1.421 (4)
Fe–C1	2.111 (3)	C1–C2	1.398 (4)	C9–C10	1.404 (4)
Fe–C2	2.044 (3)	C2–C3	1.420 (4)	P–C11	1.848 (3)
Fe–C3	2.035 (3)	C3–C4	1.418 (4)	P–C13	1.842 (3)
Fe–C4	2.070 (3)	C4–C5	1.528 (4)	P–C15	1.850 (3)
Fe–C7	2.048 (3)	C5–C6	1.544 (4)	C11–C12	1.518 (4)
Fe–C8	2.023 (3)	C6–C7	1.513 (4)	C13–C14	1.528 (5)
Fe–C9	2.035 (3)	C7–C8	1.415 (4)	C15–C16	1.518 (5)
Bond Angles					
P–Fe–C1	84.04 (9)	C4–Fe–C7	84.3 (1)	C8–C9–C10	120.1 (3)
P–Fe–C2	122.09 (8)	C4–Fe–C10	167.3 (1)	Fe–P–C11	119.1 (1)
P–Fe–C3	129.54 (9)	C7–Fe–C10	84.4 (1)	Fe–P–C13	116.88 (9)
P–Fe–C4	95.80 (8)	C1–C2–C3	119.1 (3)	Fe–P–C15	117.3 (1)
P–Fe–C7	91.79 (8)	C2–C3–C4	121.5 (2)	C11–P–C13	101.7 (1)
P–Fe–C8	129.19 (8)	C3–C4–C5	117.1 (3)	C11–P–C15	96.2 (1)
P–Fe–C9	127.46 (8)	C4–C5–C6	112.0 (3)	C13–P–C15	102.2 (1)
P–Fe–C10	90.33 (8)	C5–C6–C7	111.2 (2)	P–C11–C12	117.9 (2)
C1–Fe–C4	85.7 (1)	C6–C7–C8	120.5 (2)	P–C13–C14	118.4 (2)
C1–Fe–C7	168.7 (1)	C7–C8–C9	118.9 (2)	P–C15–C16	117.0 (2)
C1–Fe–C10	106.0 (1)				

Scheme III[a]

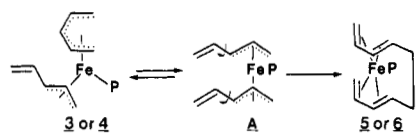

[a] P = PEt_3 or P-*n*-Pr_3.

(10) Although the coupling of pentadienyl ligands is not uncommon, the organometallic products of these reactions are usually bimetallic decatetraene complexes. See, for example: (a) Mahler, J. E.; Gibson, D. H.; Pettit, R. *J. Am. Chem. Soc.* **1963**, *85*, 3959. (b) Jotham, R. W.; Kettle, S. F. A.; Moll, D. B.; Stamper, P. *J. Organomet. Chem.* **1976**, *118*, 59. (c) Wilson, D. R.; Ernst, R. D.; Kralik, M. S. *Organometallics* **1984**, *3*, 1442. (d) Ma, H.; Weber, P.; Ziegler, M. L.; Ernst, R. D. *Ibid.* **1986**, *5*, 2009. To our knowledge, the only other mononuclear products of pentadienyl coupling reactions are (η^8-2,4,7,9-tetramethyl-1,3,7,9-decatetraene)Mn(PMe_3)[1a] and (η^5-cyclopentadienyl)Nb(2,4,7,9-tetramethyl-1,3,7,9-decatetraene) (Melendez, E.; Rheingold, A. L.; Ernst, R. D., private communication).

(11) Several examples of (η^4-butadiene)$_2$FeP complexes, where P is a phosphorus ligand, have been reported. See: Deeming, A. J. In *Comprehensive Organometallic Chemistry*; Wilkinson, G., Stone, F. G. A., Abel, E. W., Eds.; Pergamon: Oxford, 1982; Vol. 4, p 441.

(12) In contrast, one of the butadiene moieties in (η^5-cyclopentadienyl)Nb(2,4,7,9-tetramethyl-1,3,7,9-decatetraene) is bonded to the metal center in a transoid fashion while the other butadiene moiety adopts the cisoid bonding mode: Melendez, E.; Rheingold, A. L.; Ernst, R. D., private communication.

Scheme IV[a]

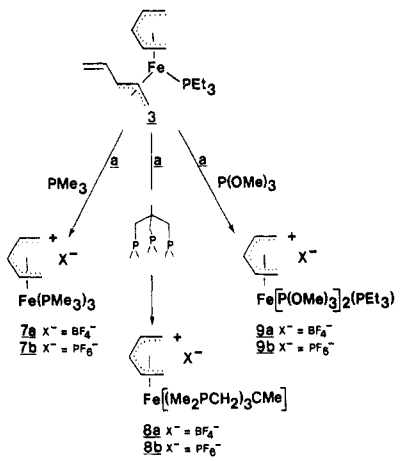

[a] (a) $HX{\cdot}OEt_2$ or Ag^+X^- ($X^- = BF_4^-$ or PF_6^-).

^1H NMR signal for H4 is highly shielded.

Compound **2** does not undergo pentadienyl coupling in refluxing diethyl ether. This observation suggests that the required 16e intermediate $(\eta^3\text{-pd})_2Fe(PR_3)$ is not accessible in the relatively uncongested PMe_3 system.

E. Synthesis of $(\eta^5$-Pentadienyl)Fe$(PMe_3)_3{}^+X^-$ (7a, $X^- = BF_4^-$; 7b, $X^- = PF_6^-$) and $(\eta^5$-Pentadienyl)Fe$[(Me_2PCH_2)_3CMe]^+X^-$ (8a, $X^- = BF_4^-$; 8b, $X^- = PF_6^-$). As indicated in Scheme IV, **3** can be converted to $(\eta^5\text{-pd})Fe(PMe_3)_3{}^+X^-$ (**7a**, $X^- = BF_4^-$; **7b**, $X^- = PF_6^-$) and $(\eta^5\text{-pd})Fe[(Me_2PCH_2)_3CMe]^+X^-$ (**8a**, $X^- = BF_4^-$; **8b**, $X^- = PF_6^-$) by two different routes—one involving protonation and the other involving oxidation. In the first approach, **3** is treated with $HBF_4{\cdot}OEt_2$ or $HPF_6{\cdot}OEt_2$ at low temperature (−78 °C) in OEt_2, stirred briefly, treated with the phosphine reagent, and then warmed to room temperature. The product salt, **7** or **8**, precipitates out of the reaction solution as a yellow solid. This reaction probably proceeds by rapid migration of the hydride to the terminus of the η^3-pd ligand. The resulting 2,4-pentadiene ligand and the bulky PEt_3 ligand are then displaced by incoming PMe_3 or $(Me_2PCH_2)_3CMe$ ligands.[13]

Unfortunately, this synthetic approach is complicated by a side reaction: protonation of the phosphine reagent by HX. In order to minimize this side reaction, the acid is added to **3** *first* and the solution is stirred for 10 min at −78 °C before addition of the phosphine. However, the side reaction cannot be totally eliminated and the organometallic products are always contaminated with a small quantity of protonated phosphine, which must be removed by repeated crystallization or column chromatography.

A second synthetic route to **7** and **8**, which avoids the side reaction described above, involves treatment of **3** with $Ag^+BF_4^-$ or $Ag^+PF_6^-$ in the presence of PEt_3 to produce a paramagnetic intermediate, $(\eta\text{-pd})_2Fe(PEt_3)_x{}^+X^-$. This dark red intermediate is then reacted with PMe_3 or $(Me_2PCH_2)_3CMe$, causing immediate release of pentadienyl radical[14] and production of bright yellow **7** and **8**. The pentadienyl radical abstracts hydrogen from CH_2Cl_2 solvent, producing *trans*-1,3-pentadiene.[15]

The exact chemical formula of the paramagnetic red intermediate is still unknown; its extreme reactivity has thwarted our attempts to characterize it fully. However, all existing evidence suggests that it is either 17e $(\eta^5\text{-pd})(\eta^3\text{-pd})Fe(PEt_3)^+X^-$ or 17e $(\eta^3\text{-pd})_2Fe(PEt_3)_2{}^+X^-$. Consistent with these formulations is the fact that it is quantitatively converted back to **3** upon treatment with sodium naphthalenide.

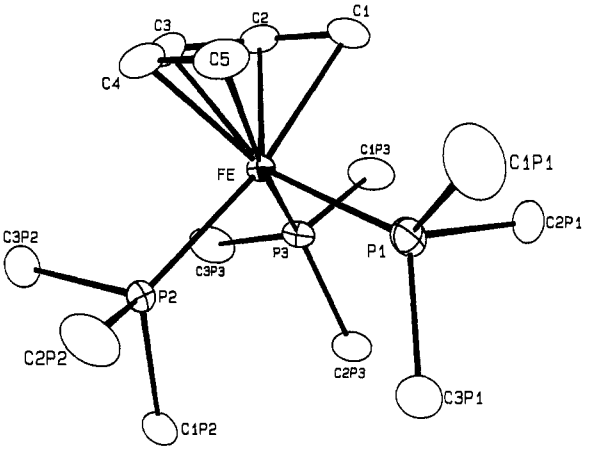

Figure 3. ORTEP drawing of $(\eta^5$-pentadienyl)Fe$(PMe_3)_3{}^+BF_4^-$ (**7a**). Hydrogen atoms are omitted for clarity.

Table V. Positional Parameters and Their Estimated Standard Deviation for Non-Hydrogen Atoms in $(\eta^5$-Pentadienyl)Fe$(PMe_3)_3{}^+BF_4^-$ (7a)

atom	*x*	*y*	*z*
Fe	0.78530 (6)	0.25107 (4)	0.16640 (3)
P1	0.6894 (2)	0.4078 (1)	0.16172 (9)
P2	0.9777 (1)	0.2805 (1)	0.09511 (8)
P3	0.6706 (1)	0.1918 (1)	0.05945 (7)
C1	0.6238 (6)	0.2050 (5)	0.2473 (3)
C2	0.7035 (6)	0.1207 (4)	0.2241 (3)
C3	0.8469 ((7)	0.1145 (5)	0.2265 (4)
C4	0.9289 (7)	0.2004 (6)	0.2529 (4)
C5	0.8793 (7)	0.2954 (6)	0.2797 (3)
C1P1	0.698 (1)	0.4851 (6)	0.2545 (5)
C2P1	0.5023 (6)	0.4151 (5)	0.1487 (4)
C3P1	0.7392 (8)	0.4988 (5)	0.0840 (5)
C1P2	0.9744 (5)	0.3200 (5)	−0.0090 (3)
C2P2	1.0907 (6)	0.3818 (7)	0.1358 (4)
C3P2	1.0920 (7)	0.1689 (7)	0.0855 (5)
C1P3	0.4969 (6)	0.1415 (6)	0.0755 (4)
C2P3	0.6301 (6)	0.2770 (5)	−0.0244 (3)
C3P3	0.7494 (8)	0.0832 (5)	0.0080 (4)
B	0.2901 (7)	0.3177 (5)	0.3564 (4)
F1	0.2979 (4)	0.2541 (3)	0.4208 (2)
F2	0.4066 (3)	0.3793 (3)	0.3568 (2)
F3	0.2828 (5)	0.2601 (4)	0.2891 (3)
F4	0.1737 (4)	0.3777 (4)	0.3635 (3)

F. Structure of $(\eta^5$-Pentadienyl)Fe$(PMe_3)_3{}^+BF_4^-$ (7a). Dynamics of $(\eta^5$-Pentadienyl)Fe$(PMe_3)_3{}^+X^-$ (7) and $(\eta^5$-Pentadienyl)Fe$[(Me_2PCH_2)_3CMe]^+X^-$ (8). The molecular structure of **7a** (Figure 3) has been determined by single-crystal X-ray diffraction. Positional parameters of the non-hydrogen atoms are listed in Table V, while selected bond distances and angles are given in Table VI. The geometry of the cation in **7a** is pseudooctahedral with C1, C3, and C5 of the pd ligand and the three phosphorus atoms of the phosphine ligands occupying the six coordination sites. Phosphorus atom P1 is bent up into the "mouth" of the pd ligand and lies substantially closer to

(13) We have used similar protonation reactions to produce $(\eta^5\text{-pd})Fe(PMe_3)_3{}^+O_3SCF_3^-$ from $(\eta^3\text{-pd})_2Fe(PMe_3)_2$ and $(\eta^5\text{-2,4-Me}_2\text{pd})Fe(PMe_3)_3{}^+O_3SCF_3^-$ from $(\eta^5\text{-2,4-Me}_2\text{pd})(\eta^3\text{-2,4-Me}_2\text{pd})Fe(PMe_3)$. See ref 1k and 1i.

(14) Extrusion of a pentadienyl radical from a paramagnetic 17e pd–M complex has precedent in cobalt chemistry. Earlier, we reported that $(\eta^5\text{-Me}_2\text{pd})Co(PEt_3)_2{}^+$, $(\eta^3\text{-2,4-Me}_2\text{pd})Co(PMe_3)_3{}^+$, and $(\eta^5\text{-2,4-Me}_2\text{Pd})Co(PEt_3)(I)$—all 17e Co(II) complexes—react cleanly with $P(OMe)_3$ to release pentadienyl radical and generate 18e Co(I) complexes. See ref 1e.

(15) This product was detected by gas chromatography, using a 12 ft. × 1/8 in. column containing 3% OV-1 on Chrom-W-HP, an oven temperature of 30 °C, and a carrier gas flow rate of 19 mL/min.

Table VI. Bond Distances (Å) and Bond Angles (deg) with Estimated Standard Deviations for (η^5-Pentadienyl)Fe(PMe_3)$_3^+BF_4^-$ (7a)

Bond Distances

Fe–P1	2.229 (1)	Fe–C5	2.183 (5)	P1–C2P1	1.828 (7)	P3–C2P3	1.830 (6)
Fe–P2	2.259 (1)	C1–C2	1.394 (8)	P1–C3P1	1.827 (7)	P3–C3P3	1.822 (6)
Pe–P3	2.243 (1)	C2–C3	1.393 (8)	P2–C1P2	1.826 (5)	B–F1	1.362 (7)
Fe–C1	2.168 (5)	C3–C4	1.43 (1)	P2–C2P2	1.837 (8)	B–F2	1.382 (6)
Fe–C2	2.103 (5)	C4–C5	1.39 (1)	P2–C3P2	1.827 (7)	B–F3	1.357 (6)
Fe–C3	2.118 (5)	P1–C1P1	1.855 (8)	P3–C1P3	1.828 (6)	B–F4	1.376 (6)
Fe–C4	2.111 (6)						

Bond Angles

P1–Fe–P2	100.05 (5)	C3–Fe–C5	71.8 (3)	C1P2–P2–C3P2	98.1 (3)
P1–Fe–P3	94.46 (5)	C1–C2–C3	126.3 (6)	C2P2–P2–C3P2	103.6 (5)
P2–Fe–P3	92.13 (4)	C2–C3–C4	121.0 (6)	Fe–P3–C1P3	117.0 (2)
P1–Fe–C1	88.2 (2)	C3–C4–C5	126.1 (7)	Fe–P3–C2P3	121.0 (2)
P1–Fe–C3	152.8 (2)	Fe–P1–C1P1	116.4 (4)	Fe–P3–C3P3	116.0 (3)
P1–Fe–C5	87.9 (2)	Fe–P1–C2P1	117.7 (2)	C1P3–P3–C2P3	97.8 (3)
P2–Fe–C1	169.8 (2)	Fe–P1–C3P1	119.8 (2)	C1P3–P3–C3P3	100.8 (4)
P2–Fe–C3	99.4 (2)	C1P1–P1–C2P1	96.2 (5)	C2P3–P3–C3P3	100.7 (3)
P2–Fe–C5	94.5 (2)	C1P1–P1–C3P1	104.3 (5)	F1–B–F2	107.7 (5)
P3–Fe–C1	93.1 (2)	C2P1–P1–C3P1	98.5 (4)	F1–B–F3	109.7 (5)
P3–Fe–C3	103.6 (2)	Fe–P2–C1P2	123.3 (2)	F1–B–F4	108.1 (5)
P3–Fe–C5	172.4 (2)	Fe–P2–C2P2	114.5 (3)	F2–B–F3	111.0 (5)
C1–Fe–C3	70.9 (3)	Fe–P2–C3P2	114.8 (2)	F2–B–F4	110.2 (4)
C1–Fe–C5	79.7 (2)	C1P2–P2–C2P2	99.5 (3)	F3–B–F4	110.2 (5)

the pd plane than P2 and P3 (2.30 Å vs 2.87 and 2.91 Å).[16]

In solution, both **7** and **8** adopt pseudooctahedral coordination geometries. Hence, the stopped-exchange ^1H

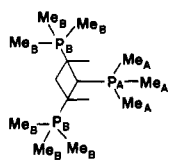

7

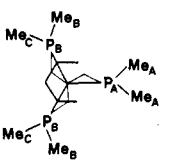

8

and $^{13}C\{^1H\}$ NMR spectra of **7** exhibit two signals for the phosphine methyls—one for the "mouth" methyls (A, intensity 1) and one for the "edge" methyls (B, intensity 2). Similarly, **8**'s stopped-exchange NMR spectra exhibit three equal-intensity signals for the phosphine methyls—one for the "mouth" methyls (A), one for the outer "edge" methyls (B), and one for the inner "edge" methyls (C).

However, as samples of **7** and **8** are heated in solution, the pentadienyl ligands begin to rotate with respect to the phosphine ligands, causing exchange of the phosphine methyl groups and, ultimately, coalescence of their NMR signals.[17] Line-shape simulations of the variable-temperature NMR spectra yield $\Delta G^{\ddagger}$'s for exchange of 17.7 ± 0.4 kcal for **7** and 13.9 ± 0.5 kcal for **8**.

G. Synthesis of (η^5-Pentadienyl)Fe[P(OMe)$_3$]$_2$(PEt$_3$)$^+X^-$ (9). Treatment of **3** with $HX{\cdot}OEt_2$ or Ag^+X^-, followed by addition of $P(OMe)_3$, leads to the synthesis of the mixed-ligand complex (η^5-pd)Fe[P(OMe)$_3$]$_2$(PEt$_3$)$^+X^-$ (**9a**, $X^- = BF_4^-$; **9b**, $X^- = PF_6^-$). Mechanistically, these phosphite reactions probably proceed in much the same way as those involving phosphine reagents (cf. section E).

In solution, **9** exists as a 80:20 equilibrium mixture of two isomers. The major isomer, labeled A, has an unsymmetrical structure in which one $P(OMe)_3$ ligand resides under the pd "mouth", while the other $P(OMe)_3$ ligand and the PEt_3 ligand occupy "edge" sites. In the minor isomer (B), the $P(OMe)_3$ ligands reside in equivalent "edge" sites, while the PEt_3 ligand sits under the open "mouth".

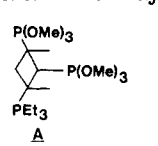

A

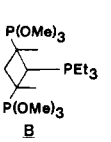

B

H. Dynamics of (η^5-Pentadienyl)Fe[P(OMe)$_3$]$_2$(PEt$_3$)$^+X^-$ (9). As **9** is heated in solution, two distinct dynamic processes can be observed by NMR. First, the two phosphite ligands in isomer A are exchanged by the pentadienyl ligand rotation shown.

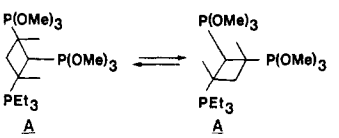

A A

In this process, which has a $\Delta G^{\ddagger}$ of 13.7 ± 0.2 kcal/mol, the two $P(OMe)_3$ ligands alternate in the "mouth" position while the PEt_3 ligand remains under the pd backbone.

At higher temperatures, isomers A and B exchange via the pentadienyl ligand rotation shown. Under these

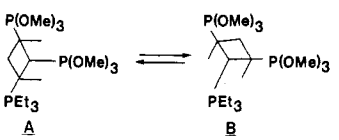

A B

conditions, all three ligands alternately occupy the "mouth" position. The $\Delta G^{\ddagger}$ for this process, as calculated from the coalescence behavior of the ^{13}C NMR signals due to the PEt_3 ligands in A and B, is 15.8 ± 0.2 kcal/mol.

Experimental Section

A. General Data. All manipulations were carried out under inert atmosphere, using either drybox or Schlenk techniques. Diethyl ether and tetrahydrofuran were dried with sodium/benzophenone and distilled before use. Pentane was dried over calcium hydride and distilled. Dichloromethane was dried over magnesium sulfate and distilled. Acetonitrile was refluxed over P_2O_5 and distilled. 1,1,1-Tris(chloromethyl)ethane and tetramethyldiphosphine disulfide (for the synthesis of $(Me_2PCH_2)_3CMe$) were purchased from Organometallics, Inc. (East Hampstead, NH), and Pressure Chemical Co., respectively, and used as received. Anhydrous iron(II) chloride (Thiokol, Alfa Products), $HBF_4{\cdot}OEt_2$ (Aldrich), $HPF_6{\cdot}OEt_2$ (Columbia), $Ag^+BF_4^-$ (Aldrich), $Ag^+PF_6^-$ (Aldrich), PMe_3 (Strem), PEt_3 (Strem), P-*n*-Pr_3

(16) The structural features of the cation in **7a** closely resemble those of the cation in (η^5-2,4-Me_2pd)Fe(PMe_3)$_3^+FeCl_3(PMe_3)^-$, which we reported earlier. See ref 1i.

(17) We have observed similar fluxional behavior for (η^5-pd)MnP_3,[1f] (η^5-pd)ReP_3,[1g] and (η^5-pd)FeP_3^+[1i,k] complexes.

(Strem), and $P(OMe)_3$ (Aldrich) were all used without further purification. $(Me_2PCH_2)_3CMe$ was synthesized via the procedure of Whitesides,[18] except for the following modification, which was suggested by K. Caulton and R. Geerts (Indiana University): Me_2PPMe_2, an intermediate in the synthesis, was obtained by heating a mixture of $Me_2P(S)P(S)Me_2$ and iron metal with a natural gas–oxygen torch. Potassium pentadienide–tetrahydrofuran was prepared by the method of Nakamura.[19] Sodium naphthalenide was produced by direct reaction of sodium with naphthalene in tetrahydrofuran. $(\eta^3$-Pentadienyl$)_3Fe(PMe_3)_2$ was prepared by the literature method.[1b]

NMR experiments were performed on a Varian XL-300 NMR spectrometer. ^1H (300 MHz) and ^{13}C (75 MHz) spectra were referenced to tetramethylsilane. ^{31}P spectra (121 MHz) were referenced to external H_3PO_4. In general, ^{13}C NMR peak assignments were made from gated decoupled spectra. ^1H NMR peak assignments were then obtained from ^{13}C–^1H shift-correlated (HETCOR) 2D spectra. Some connectivities were ascertained from ^1H–^1H and ^{31}P–^{31}P shift-correlated (COSY) 2D spectra. Infrared spectra were recorded on a Perkin-Elmer 283B spectrophotometer. Microanalyses were performed by Galbraith Laboratories, Inc., Knoxville, TN.

B. Synthesis of (η^5-Pentadienyl)(η^3-pentadienyl)Fe(PMe_3) (2). $(\eta^3$-pd$)_2Fe(PMe_3)_2$ (0.30 g, 8.8×10^{-4} mol) (1) was refluxed in 60 mL of diethyl ether for 2 days. The solvent was removed under reduced pressure leaving a dark red solid and a small amount of iron metal due to decomposition. The red solid was then extracted with a minimal amount of pentane and filtered through Celite. Dark red crystals were obtained from a saturated pentane solution at −30 °C: yield of crystalline product, 0.093 g (40%); ^1H NMR (20 °C, benzene-d_6) δ 5.75 (d of t, 1, H9), 5.02–4.81 (m, 3, H3, H10's), 4.29 (d of q, 1, H7), 3.98 (d of q, 1, H4), 3.77 (d of q, 1, H2), 2.34 (t, 1, $H5_{syn}$), 2.26 (t, 1, $H1_{syn}$), 1.30 (d, 1, $H6_{syn}$), 1.19 (d, J_{P-H} = 7.8 Hz, 9, phosphine CH_3's), 0.93–0.80 (m, 1, H8), −0.33 (d of d, 1, $H6_{anti}$), −0.45 (d of d, 1, $H5_{anti}$), −0.75 (d of d, 1, $H1_{anti}$); $^{13}C\{^1H\}$ NMR (20 °C, benzene-d_6) δ 145.2 (C9), 106.6 (C10), 94.7 (C3), 93.8 (d, J_{P-C} = 2.7 Hz, C4), 90.6 (C2), 78.5 (C7), 54.6 (d, J_{P-C} = 4.6 Hz, C8), 50.1 (d, J_{P-C} = 13.6 Hz, C5), 48.0 (d, J_{P-C} = 12.6 Hz, C1), 33.4 (d, J_{P-C} = 7.6 Hz, C6), 20.0 (d, J_{P-C} = 27 Hz, phosphine CH_3's); $^{31}P\{^1H\}$ NMR (20 °C, benzene-d_6) δ 27.2; IR (toluene, selected peaks) 1609 (C=C stretch), 1028 cm^{-1} (P—C stretch). Anal. Calcd for $C_{13}H_{23}FeP$: C, 58.66; H, 8.73. Found: C, 58.55; H, 8.53.

C. Synthesis of (η^5-Pentadienyl)(η^3-pentadienyl)Fe(PEt_3) (3). $FeCl_2$ (2.5 g, 0.020 mol) and PEt_3 (7.1 g, 0.060 mol) in 250 mL of THF were refluxed for 2 h. The solution was then stirred at room temperature for an additional 12 h and filtered through Celite on a fine frit, yielding a pale green solution of $FeCl_2(PEt_3)_2$. The solution was then cooled to −78 °C, and potassium pentadienide–tetrahydrofuran (7.13 g, 0.040 mol) in 200 mL of THF was added dropwise over a period of 1 h. After the addition was complete, the solution was allowed to warm slowly to room temperature and filtered through Celite. The solvent was removed under vacuum, leaving a dark red solid which was then extracted with pentane. The resultant solution was then filtered through Celite, concentrated, and cooled to −30 °C. The product crystallized as dark red blocks. Second and third crops were obtained by concentrating the mother liquor and cooling to −30 °C: yield of crystalline product, 4.1 g (67%). ^1H NMR (20 °C, benzene-d_6) δ 5.84 (m, 1, H9), 5.02–4.91 (m, 3, H3, H10's), 4.34 (br q, 1, H7), 4.09 (br q, 1, H4), 3.79 (br q, 1, H2), 2.68 (br t, 1, $H5_{syn}$), 2.44 (br t, 1, $H1_{syn}$), 1.57 (t, 6, phosphine CH_2's), 1.46 (m, 1, $H6_{syn}$), 0.96–0.87 (m, 9, phosphine CH_3's), 0.76 (q, 1, H8), −0.45 (t, 1, $H6_{anti}$), −0.56 (br m, 1, $H5_{anti}$), −0.99 (br m, 1, $H1_{anti}$); $^{13}C\{^1H\}$ NMR (20 °C, benzene-d_6) δ 145.2 (s, C9), 106.2 (s, C10), 94.7 (s, C3), 94.4 (s, C4), 90.7 (s, C2), 79.2 (s, C7), 53.8 (s, C8), 48.6 (s, C5), 45.9 (s, C1), 33.2 (s, C6), 19.4 (d, phosphine CH_2's), 8.58 (s, phosphine CH_3's); $^{31}P\{^1H\}$ NMR (20 °C, benzene-d_6) δ 53.8; IR (benzene, selected peaks) 1609 (C=C stretch), 1028 cm^{-1} (P—C stretch). Anal. Calcd for $C_{16}H_{29}FeP$: C, 62.34; H, 9.50. Found: C, 62.04; H, 9.08.

D. Synthesis of (η^5-Pentadienyl)(η^3-pentadienyl)Fe(P-*n*-Pr_3) (4). $FeCl_2$ (2.5 g, 0.020 mol) and P-*n*-Pr_3 (9.6 g, 0.060 mol) in 250 mL of THF were refluxed for 2 h. The solution was then stirred at room temperature for an additional 12 h and filtered through Celite on a fine frit, yielding a pale green solution of $FeCl_2$(P-*n*-$Pr_3)_2$. This solution was then cooled to −78 °C, and potassium pentadienide–tetrahydrofuran (7.13 g, 0.040 mol) in 200 mL of THF was added dropwise over the period of 1 h. After the addition was complete, the solution was allowed to warm to room temperature and filtered through Celite. The solvent was removed under vacuum, leaving a dark red solid which was extracted with pentane. The resultant solution was then filtered through Celite, concentrated, and cooled to −30 °C. The product crystallized as dark red blocks: yield of crystalline product, 4.2 g (60%); ^1H NMR (20 °C, benzene-d_6) δ 5.85 (d of t, 1, H9), 5.03–4.90 (m, 3, H3, H10's), 4.36 (q, 1, H7), 4.12 (q, 1, H4), 3.90 (q, 1, H2), 2.71 (t, 1, $H5_{syn}$), 2.47 (t, 1, $H1_{syn}$), 1.69–1.61 (m, 6, phosphine CH_2's), 1.50–1.39 (m, 6, phosphine CH_2's), 1.28–1.19 (m, 1, $H6_{syn}$), 0.90 (m, 10, H8, phosphine CH_3's), −0.35–(−1.10) (m, 2, $H6_{anti}$, $H5_{anti}$), −0.90 (d of d, 1, $H1_{anti}$); $^{13}C\{^1H\}$ NMR (20 °C, benzene-d_6) δ 145.5 (C9), 106.4 (C10), 94.9 (C3), 94.6 (C4), 90.1 (C2), 79.7 (C7), 54.0 (C8), 49.2 (C5), 46.3 (C1), 33.3 (C6), 30.1 (d, phosphine CH_2's), 19.0 (d, phosphine CH_2's), 16.4 (phosphine CH_3's); $^{31}P\{^1H\}$ NMR (20 °C, benzene-d_6) δ 46.20; IR (toluene, selected peaks) 1610 (C=C stretch), 1070 cm^{-1} (P—C stretch). Anal. Calcd for $C_{19}H_{35}FeP$: C, 65.13; H, 10.09. Found: C, 65.08; H, 9.98.

E. Reactions of 3 and 4 with PMe_3. Synthesis of (η^3-Pentadienyl)$_2$Fe($PMe_3)_2$ (1). Trimethylphosphine (0.38 g, 5.0 $\times 10^{-3}$ mol) in 10 mL of diethyl ether was added to 3 (0.31 g, 1.0 $\times 10^{-3}$ mol) or 4 (0.35 g, 1.0×10^{-3} mol) in 50 mL diethyl ether, and the resulting solutions were refluxed for 18 h. After removal of the solvent under vacuum, the dark red residue was extracted with pentane, filtered through Celite, and evaporated to dryness, leaving the red product (η^3-pentadienyl$)_2Fe(PMe_3)_2$: yield, 0.28 g (82%) and 0.25 g (71%) for 3 and 4, respectively. The NMR spectra of this product were identical with those of (η^3-pentadienyl$)_2Fe(PMe_3)_2$ reported earlier.

F. Synthesis of (*trans,trans*-η^8-1,3,7,9-Decatetraene)Fe(PEt_3) (5). Compound 3 (0.62 g, 2.0×10^{-3} mol) was refluxed in 100 mL of diethyl ether for 4 days. After removal of the solvent under vacuum, the orange residue was dissolved in pentane and passed through a glass frit packed with Celite and alumina. Unreacted 3 remained on the packed frit, while 5 passed through. The pentane solution of 5 was then reduced in volume and cooled to −30 °C, causing 5 to crystallize as light red blocks; yield of crystalline product, 0.42 g (68%); ^1H NMR (17 °C, benzene-d_6) δ 4.63 (m, 2, H2/H9), 4.02 (d of d, J_{H-H} = 6 Hz, J_{H-H} = 6 Hz, 2, H3/H8), 2.11 (m, 2, $H5_{syn}/H6_{syn}$), 1.77 (d of q, J_{H-H} = 7.5 Hz, J_{H-P} = 7.5 Hz, 6, phosphine CH_2's), 1.68 (d, J_{H-H} = 7.5 Hz, 2, $H5_{anti}/H6_{anti}$), 1.16 (d, J_{H-H} = 6 Hz, 2, $H1_{syn}/H10_{syn}$), 0.99 (d of t, J_{H-H} = 7.5 Hz, J_{H-P} = 12 Hz, 9, phosphine CH_3's), 0.25 (m, 2, H4/H7), −0.97 (d of d, J_{H-H} = 9 Hz, J_{H-P} = 15 Hz, 2, $H1_{anti}/H10_{anti}$); $^{13}C\{^1H\}$ NMR (17 °C, benzene-d_6) δ 83.6 (s, C3/C8), 81.4 (s, C2/C9), 59.9 (d, J_{P-C} = 8 Hz, C4/C7), 36.8 (s, C5/C6), 36.4 (d, J_{P-C} = 13 Hz, C1/C10), 19.8 (d, J_{P-C} = 21 Hz, phosphine CH_2's), 8.9 (d, J_{P-C} = 3 Hz, phosphine CH_3's); $^{31}P\{^1H\}$ NMR (17 °C, benzene-d_6) δ 51.2; IR (KBr pellet, selected peaks) 1460–1400, 1200 (C–C bends/stretches), 1035 cm^{-1} (P–C stretch). Anal. Calcd for $C_{16}H_{29}FeP$: C, 62.33; H, 9.50. Found: C, 62.64; H, 9.13.

G. Synthesis of (*trans,trans*-η^8-1,3,7,9-Decatetraene)Fe(P-*n*-Pr_3) (6). Compound 4 (0.70 g, 2.0×10^{-3} mol) was refluxed in 100 mL of diethyl ether for 4 days. After removal of the solvent under vacuum, the orange residue was dissolved in pentane and passed through a glass frit packed with Celite and alumina. Unreacted 4 remained on the packed frit, while 6 passed through. The solvent was then removed under reduced pressure leaving orange 6: yield of product, 0.40 g (57%); ^1H NMR (20 °C, benzene-d_6) δ 4.65 (q, 2, H2/H9), 4.01 (t, 2, H3/H8), 2.13 (m, 2, $H5_{syn}/H6_{syn}$), 1.67 (d, 2, $H5_{anti}/H6_{anti}$), 1.40 (m, 6, phosphine CH_2's), 1.25 (m, 6, phosphine CH_2's), 1.16 (d, 2, $H1_{syn}/H10_{syn}$), 0.90 (m, 9, phosphine CH_3's), 0.25 (m, 2, H4/H7), −0.95 (d of d, 2, $H1_{anti}/H10_{anti}$); $^{13}C\{^1H\}$ NMR (20 °C, benzene-d_6) δ 83.7 (s, C3/C8), 81.6 (s, C2/C9), 60.0 (d, J_{P-C} = 8 Hz, C4/C7), 36.8 (s, C5/C6), 30.5 (d, J_{P-C} = 7 Hz, C1/C10), 20.0 (d, J_{P-C} = 13 Hz, phosphine CH_2's), 18.4 (d, J_{P-C} = 2 Hz, phosphine CH_2's), 16.5

(18) Whitesides, G. M.; Casey, C. P.; Krieger, J. K. *J. Am. Chem. Soc.* **1971**, *93*, 1379.
(19) Yasuda, H.; Ohnuma, Y.; Yamauchi, M.; Tani, H.; Nakamura, A. *Bull. Chem. Soc. Jpn.* **1979**, *52*, 2036.

(d, J_{P-C} = 2 Hz, phosphine CH_3's). $^{31}P\{^1H\}$ NMR (20 °C, benzene-d_6) δ 45.5; IR (toluene, selected peaks) 1460–1400, 1200 (C–C bends/stretches), 1065 cm^{-1} (P–C stretch).

H. Synthesis of (η^5-Pentadienyl)Fe(PMe_3)$_3^+X^-$ (7a, X^- = BF_4^-; 7b, X^- = PF_6^-). Method A. HBF_4·OEt_2 (0.24 g, 1.5 × 10^{-3} mol) or HPF_6·OEt_2 (0.33 g, 1.5 × 10^{-3} mol) in 15 mL of diethyl ether was added dropwise to a cold (−78 °C), stirred solution of **3** (0.31 g, 1.0 × 10^{-3} mol) in 100 mL of diethyl ether. After the addition was complete, the solution turned from a dark red to dark green. The green solution was allowed to stir for an additional 10 min at −78 °C at which time the cold bath was removed and trimethylphosphine (0.38 g, 5.0 × 10^{-5} mol) was added. As the solution warmed to room temperature, a yellow precipitate formed. This precipitate was collected and washed with two 25-mL portions of diethyl ether and then extracted with dichloromethane. The resulting yellow solution contained both the organometallic product (**7a** or **7b**) and $HPMe_3^+X^-$; the latter was separated by repeated precipitation initiated by the addition of diethyl ether to the saturated dichloromethane solution. The product crystallized as orange cubes from a saturated THF/dichloromethane solution at −30 °C: yield of **7a**, 0.36 g (82%); yield of **7b**, 0.42 g (85%).

Method B. $AgBF_4$ (0.19 g, 1.0 × 10^{-3} mol) or $AgPF_6$ (0.25 g, 1.0 × 10^{-3} mol) in 30 mL of dichloromethane was added to a cold (−78 °C), stirred solution of **3** (0.31 g, 1.0 × 10^{-3} mol) and triethylphosphine (0.12 g, 1.0 × 10^{-3} mol) in 100 mL of dichloromethane. The resulting dark red solution was then allowed to warm to room temperature, filtered through Celite, and evacuated to dryness. The remaining solid was washed with two 25-mL portions of diethyl ether and extracted with dichloromethane. Trimethylphosphine (0.38 g, 5.0 × 10^{-5} mol) was then added and the solution immediately turned from a dark red to a bright yellow. After filtration through Celite and removal of the volatiles under vacuum, the yellow residue was redissolved in a minimal amount of a THF/dichloromethane solution and cooled to −30 °C. **7a** and **7b** crystallized as orange cubes: yield of **7a**, 0.42 g (96%); yield of **7b**, 0.47 g (95%). Anal. Calcd for **7a** ($C_{14}H_{34}FeP_3BF_4$): C, 38.38; H, 7.84. Found: C, 38.51; H, 7.82. Anal. Calcd for **7b** ($C_{14}H_{34}FeP_4F_6$): C, 33.88; H, 6.92. Found: C, 34.11; H, 6.83.

The following *stopped-exchange* spectra are obtained for **7a** and **7b**: ^1H NMR (20 °C, methylene-d_2 chloride) δ 5.83 (t, 1, H3), 4.69 (br s, 2, H2/H4), 2.14 (br s, 2, $H1_{syn}/H5_{syn}$), 1.74 (d, J_{H-P} = 8 Hz, 9, "mouth" phosphine CH_3's), 1.22 (virtual t, J_{H-P} = 8 Hz, 18, "edge" phosphine CH_3's), −0.21 (br s, 2, $H1_{anti}/H5_{anti}$); $^{13}C\{^1H\}$ NMR (20 °C, methylene-d_2 chloride) δ 97.7 (s, C2/C4), 89.1 (s, C3), 51.2 (d, C1/C5), 24.4 (d, J_{C-P} = 24 Hz, "mouth" phosphine CH_3's), 20.0 (virtual t, J_{C-P} = 26 Hz, "edge" phosphine CH_3's); $^{31}P\{^1H\}$ NMR (20 °C, methylene-d_2 chloride) a second-order AB_2 pattern with peaks at δ 16.3, 16.0, 15.9, 15.6, 14.8, 14.5, and 14.4. Line-shape analysis yielded the following chemical shifts and coupling constants: δ 15.9 ("mouth" phosphine), 14.6 ("edge" phosphines), J_{P-P} = 41 Hz. The spectrum of **7b** also contains the characteristic signal of PF_6^-: δ −144.0 (heptet, J_{P-F} = 706 Hz, 1); IR of **7a,b** (methylene chloride, selected peaks) 958, 945 cm^{-1} (P–C stretches).

I. Synthesis of (η^5-Pentadienyl)Fe[$(Me_2PCH_2)_3CMe$]$^+X^-$ (8a, X^- = BF_4^-; 8b, X^- = PF_6^-). Method A. HBF_4·OEt_2 (0.24 g, 1.5 × 10^{-3} mol) or HPF_6·OEt_2 (0.33 g, 1.5 × 10^{-3} mol) in 15 mL of diethyl ether was added dropwise to a cold (−78 °C), stirred solution of **3** (0.31 g, 1.0 × 10^{-3} mol) in 100 mL of diethyl ether. After the addition was complete, the solution turned from a dark red to dark green. The green solution was allowed to stir for an additional 10 min at −78 °C at which time the cold bath was removed and $(Me_2PCH_2)_3CMe$ (0.38 g, 1.5 × 10^{-5} mol) was added. As the solution warmed to room temperature, a yellow precipitate formed. This precipitate was collected, washed with two 25-mL portions of diethyl ether and two 25-mL portions of THF, and extracted with dichloromethane. The dichloromethane solution was then added to the top of a column packed with alumina and eluted with a mixture of dichloromethane and acetonitrile. The bright yellow band was collected. Both **8a** and **8b** crystallized from a saturated dichloromethane solution as bright yellow blocks: yield of **8a**, 0.28 g (61%); yield of **8b**, 0.30 g (57%).

Method B. $AgBF_4$ (0.19 g, 1.0 × 10^{-3} mol) or $AgPF_6$ (0.25 g, 1.0 × 10^{-3} mol) in 30 mL of dichloromethane was added to a cold (−78 °C), stirred solution of **3** (0.31 g, 1.0 × 10^{-3} mol) and triethylphosphine (0.12 g, 1.0 × 10^{-3} mol) in 100 mL of dichloromethane. The resulting dark red solution was then allowed to warm to room temperature, filtered through Celite, and evacuated to dryness. The remaining solid was washed with two 25-mL portions of diethyl ether and extracted with dichloromethane. $(Me_2PCH_2)_3CMe$ (0.38 g, 1.5 × 10^{-5} mol) was then added and the solution immediately turned from a dark red to a bright yellow. After filtration through Celite and removal of the volatiles under vacuum, the yellow residue was washed with two 25-mL portions of THF and redissolved in a minimal amount of dichloromethane and cooled to −30 °C. **8a** and **8b** crystallized as bright yellow blocks: yield of **8a**, 0.31 g (67%); yield of **8b**, 0.35 g (67%). Anal. Calcd for **8a** ($C_{16}H_{34}FeP_3BF_4$): C, 41.59; H, 7.36. Found: C, 41.54; H, 7.47. Anal. Calcd for **8b** ($C_{16}H_{34}FeP_4F_6$): C, 36.94; H, 6.59. Found: C, 36.74; H, 6.93.

The following *stopped-exchange* spectra were obtained for **8a** and **8b**. ^1H NMR (−30 °C, acetonitrile-d_3) δ 5.53 (t, J_{H-H} = 6 Hz, 1, H3), 4.77 (br s, 2, H2/H4), 2.04 (d, J_{H-H} = 9 Hz, 2, $H1_{syn}/H5_{syn}$), 1.77 (d, J_{P-H} = 9 Hz, 6, "mouth" phosphine CH_3's), 1.59 (d, J_{P-H} = 9 Hz, 2, "mouth" phosphine CH_2's), 1.40–1.17 (br s, 10, "edge" phosphine CH_3's and CH_2's), 1.32 (virtual t, J_{P-H} = 8 Hz, 6, "edge" phosphine CH_3's), 1.00 (d, J_{P-H} = 3 Hz, 3, capping CH_3), 0.36 (d, J_{H-H} = 10 Hz, 2, $H1_{anti}/H5_{anti}$); $^{13}C\{^1H\}$ NMR (−30 °C, acetonitrile-d_3) δ 97.26 (s, C2/C4), 87.64 (s, C3), 51.87 (d, J_{P-C} = 6 Hz, C1/C5), 37.27 (d, J_{P-C} = 22 Hz, "mouth" phosphine CH_2), 35.80–35.24 ("edge" phosphine CH_2's, quaternary C, capping CH_3), 24.04 (d, J_{P-C} = 31 Hz, "mouth" phosphine CH_3's), 19.80 (virtual t, J_{P-C} = 27 Hz, "edge" phosphine CH_3's), 17.00 (virtual t, J_{P-C} = 30 Hz, "edge" phosphine CH_3's); $^{31}P\{^1H\}$ NMR (−30 °C, acetonitrile-d_3) a second-order A_2B pattern with peaks at δ 31.2, 31.1, 30.7, 29.1, 28.8, 28.6, and 28.2. Line-shape analysis yielded the following chemical shifts and coupling constants: δ 30.9 ("edge" phosphines), 28.8 ("mouth" phosphine), J_{P-P} = 57 Hz. The spectrum of **8b** also contains the characteristic signal of PF_6^-: δ −144.0 (heptet, J_{P-F} = 706 Hz, 1). IR of **8a,b** (KBr pellet, selected peaks): 939, 935 cm^{-1} (P–C stretches).

J. Synthesis of (η^5-Pentadienyl)Fe[$P(OMe)_3$]$_2$(PEt_3)$^+X^-$ (9a, X^- = BF_4^-; 9b, X^- = PF_6^-). Method A. HBF_4·OEt_2 (0.24 g, 1.5 × 10^{-3} mol) or HPF_6·OEt_2 (0.33 g, 1.5 × 10^{-3} mol) in 15 mL of diethyl ether was added dropwise to a cold (−78 °C), stirred solution of **3** (0.31 g, 1.0 × 10^{-3} mol) in 100 mL of diethyl ether. After the addition was complete, the solution turned from a dark red to dark green. The green solution was allowed to stir for an additional 10 min at −78 °C at which time the cold bath was removed and $P(OMe)_3$ (0.62 g, 5.0 × 10^{-5} mol) was added. As the solution warmed to room temperature, a yellow oil formed. This oil was collected and washed with two 25-mL portions of diethyl ether and extracted with THF. The THF solution was then passed through a column packed with alumina. A yellow band was collected, and the solvent was removed under vacuum leaving a yellow oil. The oil was dissolved in 10 mL of THF, and diethyl ether was added dropwise until the solution became turbid. The solution was then filtered and cooled to −30 °C, causing the product to crystallize as yellow microcrystals: yield of **9a**, 0.53 g (92%); yield of **9b**, 0.59 g (93%).

Method B. $AgBF_4$ (0.19 g, 1.0 × 10^{-3} mol) or $AgPF_6$ (0.25 g, 1.0 × 10^{-3} mol) in 30 mL of dichloromethane was added to a cold (−78 °C), stirred solution of **3** (0.31 g, 1.0 × 10^{-3} mol) and triethylphosphine (0.12 g, 1.0 × 10^{-3} mol) in 100 mL of dichloromethane. The resulting dark red solution was then allowed to warm to room temperature, filtered through Celite, and evacuated to dryness. The remaining solid was washed with two 25-mL portions of diethyl ether and extracted with dichloromethane. $P(OMe)_3$ (0.62 g, 5.0 × 10^{-5} mol) was then added and the solution immediately turned from a dark red to a bright yellow. After filtration through Celite and removal of the volatiles under vacuum, the yellow oil was dissolved in 10 mL of THF and diethyl ether was added dropwise until the solution became turbid. The solution was then filtered and cooled to −30 °C, causing the product to crystallize as yellow microcrystals: yield of **9a**, 0.55 g (95%); yield of **9b**, 0.61 g (93%). Anal. Calcd for **9a** ($C_{17}H_{40}FeP_3O_6BF_4$): C, 35.44; H, 7.00. Found: C, 35.37; H, 6.91. Anal. Calcd for **9b** ($C_{17}H_{40}FeP_4O_6F_6$): C, 32.19; H, 6.36. Found: C, 32.30; H, 6.35.

The following *stopped-exchange* spectra are obtained for **9a** and **9b**.

Table VII. Crystal and Diffraction Data for 3, 5, and 7a

	3	5	7a
formula	$C_{16}H_{29}FeP$	$C_{16}H_{29}FeP$	$C_{14}H_{34}FeP_3BF_4$
mol wt	308.27	308.27	438.05
space group	$P\bar{1}$	$P2_1/n$	$P2_1/c$
a, Å	9.762 (6)	7.434 (4)	9.697 (2)
b, Å	10.136 (5)	27.536 (3)	12.923 (4)
c, Å	9.271 (5)	7.662 (1)	16.834 (4)
α, deg	97.95 (2)	90.0	90.0
β, deg	111.56 (4)	93.112 (3)	90.48 (2)
γ, deg	92.26 (4)	90.0	90.0
V, Å^3	840.8 (7)	1566 (1)	2109.6 (9)
Z	2	4	4
d_{calcd}, gr/cm^3	1.22	1.31	1.38
cryst color	red	bright red	orange
cryst dimens, mm	0.5 × 0.4 × 0.2	0.6 × 0.5 × 0.3	0.6 × 0.5 × 0.5
μ, cm^{-1}	9.74	10.455	9.65
abs corr	none	none	none
scan type	θ–2θ	ω	θ–2θ
scan rate, deg/min	variable (6–29)	variable (2–29)	variable (4–29)
scan width, deg	0.6	0.8	0.6
2θ min, deg	3.0	3.0	3.0
2θ max, deg	55.0	55.0	55.0
octant collected	$+h,\pm k,\pm l$	$+h,+k,\pm l$	$+h,+k,\pm l$
no. of reflcts measd	5220	3829	4736
no. of reflcts with $I > 3\sigma(I)$	3505	3041	3126
no. of parameters varied	267	250	208
data/parameter ratio	13.1	12.2	15.0
final R_F[a]	0.068	0.039	0.046
final R_{wF}[b]	0.099	0.067	0.077

[a] $R_F = \sum||F_o| - |F_c||/\sum|F_o|$. [b] $R_{wF} = [\sum w(|F_o| - |F_c|)^2/\sum w|F_o|^2]^{1/2}$; $w = 1/\sigma(|F_o|)$.

Major isomer (80%): ^{1}H NMR (–20 °C, acetonitrile-d_3) δ 6.25 (br s, 1, H3), 5.0 (br s, 2, H2/H4), 3.93 (d, J_{P-H} = 8 Hz, 9, "mouth" phosphite CH_3's), 3.69 (d, J_{P-H} = 6 Hz, 9, "edge" phosphite CH_3's), 2.43 (br s, 1, $H5_{syn}$), 2.26 (br s, 1 $H1_{syn}$), 1.60 (br s, 6, phosphine CH_2's), 1.02 (br s, 9, phosphine CH_3's), 0.10 (br s, 1, $H1_{anti}$), –0.05 (br s, 1, $H5_{anti}$); $^{13}C\{^1H\}$ NMR (–20 °C, acetonitrile-d_3) δ 97.5 (s, C2), 95.5 (s, C4), 91.4 (d, J_{P-C} = 4 Hz, C3), 54.7 (d, J_{P-C} = 10 Hz, phosphite CH_3's), 54.5 (d, J_{P-C} = 10 Hz, phosphite CH_3's), 51.9 (d of t, J_{P-C} = 13 Hz, J_{P-C} = 4 Hz, C5), 51.0 (t, J_{P-C} = 11 Hz, C1), 19.3 (d, J_{P-C} = 24 Hz, phosphine CH_2's), 8.9 (d, J_{P-C} = 5 Hz, phosphine CH_3's); $^{31}P\{^1H\}$ NMR (–20 °C, acetonitrile-d_3) δ 174.1 (d of d, J_{P-P} = 100.0 Hz, J_{P-P} = 66.8 Hz, 1, "mouth" phosphite), 160.0 (d of d, J_{P-P} = 66.8 Hz, J_{P-P} = 128.4 Hz, 1, "edge" phosphite), 37.7 (d of d, J_{P-P} = 66.8 Hz, J_{P-P} = 128.6 Hz, 1, phosphine).

Minor isomer (20%): ^{1}H NMR (–20 °C, acetonitrile-d_3) δ 6.12 (br s, 1, H3), 5.18 (br s, 2, H2/H4), 3.80–3.55 (br m, 18, phosphite CH_3's), 2.43 (br s, 2, $H1_{syn}/H5_{syn}$), 1.60 (br s, 6, phosphine CH_2's), 1.18 (br s, 9, phosphine CH_3's), 0.10 (br s, 2, $H1_{anti}/H5_{anti}$); $^{13}C\{^1H\}$ NMR (–20 °C, acetonitrile-d_3) δ 97.5 (s, C2/C4) 87.4 (s, C3), 57.4–54.5 (C1/C5), 54.3 (virtual t, J_{P-C} = 10 Hz, phosphite CH_3's), 22.7 (d, J_{P-C} = 26 Hz, phosphine CH_2's), 8.6 (d, J_{P-C} = 5 Hz, phosphine CH_3's); $^{31}P\{^1H\}$ NMR (–20 °C, acetonitrile-d_3) δ 161.6 (d, J_{P-P} = 69.3 Hz, 2, phosphites), 39.7 (t, J_{P-P} = 69.3 Hz, 1, phosphine); IR (KBr pellet, selected peaks) 1500–1410, 1175 (m, C–C bends/stretches), 1105 cm^{-1} (vs, P–O stretch).

K. X-ray Diffraction Studies of 3, 5, and 7a. Single crystals of **3**, **5**, and **7a** were sealed in glass capillaries under an inert atmosphere. Data were collected at room temperature on a Nicolet P3 diffractometer, using graphite-monochromated Mo Kα radiation. All data reduction and structure refinement were done by using the Enraf-Nonius structure determination package on a VAX 11/780 computer (modified by B.A. Frenz and Assoc., Inc., College Station, TX).[20] Crystal data and details of data collection and structure analysis are summarized in Table VII.

In each case, the structure was solved by standard Fourier techniques, following the location of the iron atom from a Patterson map. Non-hydrogen atoms were refined with anisotropic thermal parameters. For **3**, all hydrogens except those on phosphine methyl group C4P were located on difference Fourier maps and refined isotropically, while the three hydrogens on C4P were added at idealized positions and included in the structure factor calculations but not refined. For **5**, all hydrogens were located on difference Fourier maps and refined with fixed isotropic thermal parameters. For **7a**, all hydrogens were located on difference Fourier maps and included in structure factor calculations, but not refined.

L. Dynamic NMR Studies. Samples were dissolved in acetonitrile-d_3, and NMR spectra were recorded over the temperature range –30 to 60 °C. Probe temperatures were calibrated by using the temperature dependence of the difference in chemical shift between the ^{1}H resonances of the methyl and hydroxyl groups of methanol below ambient temperatures and between the ^{1}H resonances of the methylene and hydroxyl groups of ethylene glycol above ambient temperatures.[21] Theoretical line shapes were calculated for a series of rates by using the method of C. S. Johnson.[22,23] The experimental spectra (measured at various temperatures) were matched against the theoretical spectra, and, in this way, exchange rate constants were determined for each temperature. These exchange rate constants, k, were then used to calculate the free energy of activation, $\Delta G^\ddagger$, at each temperature, T, by using the Eyring equation

$$k = (k'/\hbar)Te^{-\Delta G^\ddagger/RT}$$

where k' = Boltzmann's constant, $\hbar$ = Planck's constant, and R = ideal gas constant.[24]

The partial coalescence of the ^{13}C NMR signals due to the phosphine methyl carbons was used to calculate the rotational barrier in **7**, while coalescence of the ^{13}C NMR signals due to phosphine methylene carbons was used to calculate the rotational barrier in **8**. The coalescence of the ^{13}C NMR signals due to pd carbons C1 and C5 was used to calculate the pentadienyl rotational barrier in major isomer A of **9**, while coalescence of the PEt_3 methylene carbon signals was used to calculate the $\Delta G^\ddagger$ for interconversion of major isomer A with minor isomer B of **9**.

Summary

The reaction of $FeCl_2(PMe_3)_2$ with 2 equiv of potassium pentadienide (K^+pd^-) produces (η^3-pd)$_2$Fe(PMe_3)$_2$ (**1**), which upon prolonged refluxing in diethyl ether yields (η^5-pd)(η^3-pd)Fe(PMe_3) (**2**). The PEt_3 and P-*n*-Pr_3 analogues of **2**, (η^5-pd)(η^3-pd)Fe(PEt_3) (**3**) and (η^5-pd)(η^5-pd)Fe(P-*n*-Pr_3) (**4**), are produced directly from the reactions of $FeCl_2(PR_3)_2$ with 2 equiv of K^+pd^-.

The more sterically congested complexes **3** and **4** exhibit reaction chemistry which is distinct from that of **2**. For example, **3** and **4** react with excess PMe_3 in refluxing diethyl ether to produce **1**, while **2** does not. Furthermore, when heated in the absence of PMe_3, **3** and **4** undergo pentadienyl ligand coupling to produce (η^8-1,3,7,9-decatetraene)Fe(PR_3), while **2** does not. Both of these reactions are believed to involve 16e (η^3-pd)$_2$Fe(PR_3) intermediates, which are more accessible in the more sterically crowded PEt_3 and P-*n*-Pr_3 systems.

Compound **3** serves as a convenient precursor to the electron-rich cationic complexes (η^5-pd)Fe(PMe_3)$_3^+X^-$, (η^5-pd)Fe[(Me_2PCH_2)$_3$CMe]$^+X^-$, and (η^5-pd)Fe[P(OMe)$_3$]$_2$(PEt_3)$^+X^-$. These synthetic reactions can be carried out by either protonating or oxidizing **3** and then adding the appropriate phosphine or phosphite reagent.

(20) Atomic scattering factors were obtained from the: *International Tables for X-Ray Crystallography*; Kynoch: Birmingham, England, 1974; Vol. IV.

(21) Von Geet, A. L. *Anal. Chem.* **1968**, *40*, 2227.
(22) Johnson, C. S., Jr. *Am. J. Phys.* **1967**, *35*, 929.
(23) Martin, M. L.; Martin, G. J.; Delpuech, J.-J. *Practical NMR Spectroscopy*; Heydon: London, 1980; pp 303–309.
(24) Lowry, T. H.; Richardson, K. S. *Mechanism and Theory in Organic Chemistry*; Harper and Row: New York, 1976.

In solution, the (η^5-pd)FeL_3^+ complexes undergo dynamic processes involving rotation of the pd ligand with respect to the FeL_3 fragment.

Currently, we are attempting to functionalize the decatetraene ligands in **5** and **6** and are probing the reactivity of cationic complexes **7**, **8**, and **9** toward nucleophiles. Results of these studies will be reported in the future.

Acknowledgment. Support from the National Science Foundation (Grant CHE-8520680) is gratefully acknowledged. Washington University's High Resolution NMR Service Facility was funded in part by National Institutes of Health Biomedical Research Support Instrument Grant 1 S10 RR02004 and by a gift from Monsanto Company. M.K.H. thanks the AAUW Educational Foundation for providing a Dissertation Fellowship. We thank Patricia Earl for synthesizing $(Me_2PCH_2)_3CMe$.

Registry No. **1**, 88765-93-9; **2**, 113948-15-5; **3**, 113975-07-8; **4**, 113948-16-6; **5**, 113975-08-9; **6**, 113948-17-7; **7a**, 113948-19-9; **7b**, 114029-28-6; **8a**, 113948-21-3; **8b**, 114029-27-5; **9a** (isomer A), 114029-31-1; **9a** (isomer B), 114127-19-4; **9b** (isomer A), 113948-24-6; **9b** (isomer B), 114029-30-0; K^+Pd^-, 51391-25-4; $FeCl_2(PEt_3)_2$, 95075-11-9; $FeCl_2(P(n\text{-}Pr)_3)_2$, 113948-22-4; PMe_3, 594-09-2; $(Me_2PCH_2)_3CMe$, 77609-83-7; $P(OMe)_3$, 121-45-9.

Supplementary Material Available: Listings of final atomic coordinates, thermal parameters, bond lengths, bond angles, and significant least-squares planes for **3**, **5**, and **7a** (19 pages); listings of observed and calculated structure factor amplitudes for **3**, **5**, and **7a** (36 pages). Ordering information is given on any current masthead page.

Electronic Structures and EPR Spectra of Carbonylbis(cyclopentadienyl)vanadium(II) and Carbonylbis(pentadienyl)vanadium(II)

Ruth M. Kowaleski,† Fred Basolo,† Joseph H. Osborne,‡ and William C. Trogler*,‡

Department of Chemistry, Northwestern University, Evanston, Illinois 60201, and Department of Chemistry, D-006, University of California at San Diego, La Jolla, California 92093

Received December 22, 1987

The electronic structures of Cp_2V and pd_2V, where Cp = η-C_5H_5 and pd = η-C_5H_7, have been modeled by spin-restricted and spin-polarized SCF–Xα–DV calculations. In agreement with the experimental magnetic moments Cp_2V is calculated to adopt a high spin (three unpaired electrons) ground electronic state and pd_2V contains one unpaired electron. While the d orbitals in Cp_2V split in a pseudooctahedral pattern those in pd_2V show a considerable distortion and splitting. Calculations for the carbonyl adducts Cp_2VCO and pd_2VCO show the highest occupied orbital is $12a_1$ in both cases, which yields a $^2A_1$ ground state. The vanadium atom is calculated to be more positively charged in the pd derivative and this conforms to the 80 cm^{-1} higher IR CO stretching frequency in this complex. Radical reactivity depends critically on the $12a_1$ orbital. In Cp_2VCO orbital contour plots show the odd electron in a a_1 d orbital hybrid localized between the two cyclopentadienyl ring planes; however, in pd_2VCO the $12a_1$ orbital is calculated to point toward the center of the pd ligands. The EPR spectra of the complexes pd_2VCO, pd'_2VCO, Cp(pd)VCO, Cp(pd')VCO, Cp_2VCO, and Cp^*_2VCO (where Cp* = η-$C_5(CH_3)_5$ and pd' = 2,4-$(CH_3)_2C_5H_5$) and their ^{13}CO derivatives at room temperature and in frozen methylcyclohexane are reported. The isotropic coupling constants for this series of complexes range from -7.36×10^{-3} cm^{-1} (79.1 G) for pd_2VCO to -1.73×10^{-3} cm^{-1} (18.6 G) for Cp^*_2VCO. The EPR parameters indicate greater covalency and lower charge on vanadium in the cyclopentadienyl complexes as compared to the pentadienyl complexes and support the conclusions of the SCF–Xα–DV calculations. Small hyperfine splittings from delocalization of the unpaired electron onto the CO ligand were observed for $Cp_2V^{13}CO$ and $Cp^*_2V^{13}CO$ (A^C_{iso} = 9.3×10^{-4} and 10.7×10^{-4} cm^{-1}, respectively). No evidence for delocalization onto the CO ligand could be found in the complexes containing pentadienyl ligands.

Introduction

Electronic structures of 17-electron complexes might contain information to help one understand the enhanced reactivity of these complexes as compared to their 18-electron analogues. Studies of 17-electron metal carbonyl complexes such as $V(CO)_6$, $Mn(CO)_5$, $Fe(CO)_3(PR_3)_2^+$, and $(\eta^4$-$C_4H_6)_2MnCO$ suggest the extent of delocalization of the unpaired electron onto the ligands and the directional properties of the singly occupied molecular orbital (SOMO) may help to explain the associative substitution lability of these complexes.[1-5] One thesis we have favored[5] is stabilization of 19-electron transition states or intermediates by bonding between a pair of electrons on an attacking nucleophile and an orbital on the metal that is half-occupied in the radical.

The 17-electron vanadocene derivatives (η^5-L)$_2$VCO (η^5-L = Cp = C_5H_5, Cp* = C_5Me_5, pd' = 2,4-$Me_2C_5H_5$, and

† Northwestern University.
‡ University of California at San Diego.

(1) Bratt, S. W.; Kassyk, A.; Perutz, R. N.; Symons, M. C. R. *J. Am. Chem. Soc.* **1982**, *104*, 490–494.
(2) (a) McCall, J. M.; Morton, J. R.; Preston, K. F. *J. Magn. Reson.* **1984**, *64*, 414–419. (b) Howard, J. A.; Morton, J. R.; Preston, K. F. *Chem. Phys. Lett.* **1981**, *83*, 226–228.
(3) Herrinton, T. R.; Brown, T. L. *J. Am. Chem. Soc.* **1985**, *107*, 5700–5703.
(4) Harlow, R. L.; Krusic, P. J.; McKinney, R. J.; Wreford, S. S. *Organometallics* **1982**, *1*, 1506–1513.
(5) (a) Holland, G. F.; Manning, M. C.; Ellis, D. E.; Trogler, W. C. *J. Am. Chem. Soc.* **1983**, *105*, 2308–2314. (b) Shi, Q.-Z.; Richmond, T. G.; Trogler, W. C.; Basolo, F. *Ibid.* **1982**, *104*, 4032–4034; **1984**, *106*, 71–76. (c) Therien, M. J.; Trogler, W. C. *Ibid.* **1986**, *108*, 3697–3702. (d) Therien, M. J.; Ni, C. L.; Anson, F. C.; Osteryoung, J. G.; Trogler, W. C. *Ibid.* **1986**, *108*, 4037–4042. (e) Trogler, W. C. *Int. J. Chem. Kinet.* **1987**, *19*, 1025–1047.

0276-7333/88/2307-1425$01.50/0